Control of the turbulent wake flow behind a circular cylinder by asymmetric sectoral hydrophobic coatings

Anatoliy Lebedev[1], Konstantin Dobroselsky[1], Alexey Safonov[1], Sergey Starinskiy[1,2], Veronica Sulyaeva[3], Aleksei Lobasov[1], Vladimir Dulin[1,2,*], Christos N. Markides[1,4]

[1] Kutateladze Institute of Thermophysics,
1 Lavrentyev Avenue, Novosibirsk, 630090, Russia

[2]Department of Physics, Novosibirsk State University,
2 Pirogova Street, Novosibirsk, 630090, Russia

[3] Nikolaev Institute of Inorganic Chemistry,
3 Lavrentyev Avenue, Novosibirsk, 630090, Russia

[4]Clean Energy Processes (CEP) Laboratory, Department of Chemical Engineering,
Imperial College London, South Kensington Campus, London SW7 2AZ, United Kingdom

* **Corresponding author.** Email: vmd@itp.nsc.ru

N.B.: This is the ACCEPTED version of this article. The final, published version of the article can be found at: https://doi.org/10.1063/5.0073687

Abstract

We demonstrate that sectoral coating by a hydrophobic fluoropolymer is an effective method for controlling flow separation and the turbulent wake behind a cylinder in high Reynolds number flows ($Re = 2.2 \times 10^5$). Time-resolved particle image velocimetry measurements show that the shape of the wake and trajectory of large-scale vortex structures are inclined due to delayed flow separation on one side of the cylinder. Near-wall, high-resolution visualization reveals that this effect is related to micro-bubbles travelling along the coated surface. The properties of the coatings and bubble presence did not deteriorate, even after many hours of continuous facility operation.

Surfaces with superhydrophobic properties, obtained by micro-structuring hydrophobic materials, can be used as an effective solution to different problems, including drag reduction, anti-corrosion, anti-icing, self-cleaning and others (Rothstein, 2010; Golovin et al., 2016; Kim and Lee, 2017). In addition to inducing or controlling roughness effects over completely wetted surfaces, trapped air pockets between relief irregularities result in flow slip, which has been shown to provide sufficient reduction of viscous drag (Daniello et al., 2009; Aljallis et al., 2013; Park and Sun, 2014; Gose et al. 2018; Bullee et al. 2020). However, the drag reduction effect typically decreases in higher Reynolds number flows and can vanish when the flow becomes fully turbulent. Whereas drag reduction is still possible at high Reynolds numbers when the texture roughness elements are oriented along the flow (Golovin et al. 2016), a fundamental limitation is expected in turbulent flows due to local surface wetting when the fluctuations of pressure exceed the capillary resistance of the coating. The longevity of the superhydrophobic surface effect is crucial in practical applications, because the removal of the air pockets from the surface can result in a significant deterioration in the expected degree of drag reduction and even in an increase in drag.

Beyond uniformly affecting the surface properties of solid surfaces, altering these properties over the surfaces (i.e., by establishing separate hydrophobic/hydrophilic regions) is also an effective strategy for flow control, specifically by affecting flow separation and vortex shedding over bluff bodies, e.g., circular cylinders (You and Moin, 2007; Legendre et al. 2009; Selimefendigil and Öztop, 2014; Mastrokalos et al., 2015 Mastrokalos and Kaiktsis, 2017; Huang et al, 2018; Wen et al., 2018). Recently in this context, Sooraj et al. (2020) reported on the effect of hydrophilicity and superhydrophobicity on the flow dynamics around a circular cylinder for flows with Reynolds numbers in the range Re = 45 − 15 500 by using particle image velocimetry (PIV). The recirculation zone length and the energy of coherent velocity fluctuations, induced by vortex shedding was found in this work to reduce with Re. Furthermore, Muralidhar et al. (2011) reported that the streamwise orientation of ridges over a superhydrophobic surface can result in an upstream shift of the separation angle location for Re typically below 10^4 and higher vortex shedding frequencies for even lower Re. For flows in the range Re = $7 \times 10^3 - 2.3 \times 10^4$, Kim et al. (2015) first observed that a superhydrophobic rough coating can shift the separation point downstream, leading to a smaller recirculation zone (i.e., reduced length by up to 40%) and a reduction in drag, but also that this effect reversed at higher Re. Interestingly, the same authors demonstrated the potential of localised coating around the separation point to control the flow.

Motivated by the aforementioned experimental studies of hydrophobicity effects in flows around circular cylinders, the present study aims to demonstrate that local sectoral coatings can be used for the effective control of flow separation and of the dynamics of large-scale vortex structures in high Reynolds number (Re = 2.2×10^5) flows over circular cylinders. The investigation is based on the application of time-resolved PIV and includes direct comparisons to the case of a completely coated cylinder. We determine that the asymmetric orientation of the transversal layers of the hydrophobic/non-hydrophobic surfaces with respect to the flow direction can sufficiently incline the flow wake and increase the kinetic energy of the flow fluctuations.

Because superhydrophobic coatings are prone to degradation, there is a shortlist of materials that allow them to retain their hydrophobic properties in practical applications. One of these materials is a fluoropolymer (Wal, 2007; Aktas, 2019), which was used to create sustainable hydrophobic surfaces in the present study. Figure 1 shows schematics of the manufacture of experimental samples. The cylinders with a diameter d = 26 mm were made of stainless steel (AISI 321). They were covered by a fluoropolymer layer with the thickness of approximately 500 nm by using a hot wire chemical vapor deposition method (Safonov et al., 2018), adapted by Safonov et al. (2020) and Bykov et al. (2021). The contact angle for the water droplets on the coated surface was measured and found to be $124 \pm 2°$ by a DSA-100 KRUSS device (see Figure 1c).

The fluoropolymer coating on the cylinders was locally removed by ablating the coating by using the second harmonic (532 nm) of a pulsed Nd:YAG laser (Figure 1a) to obtain lateral sectors with non-hydrophobic properties. The fluence of a focused laser spot was 0.3 J/cm^2. The laser treatment almost completely removes the fluoropolymer coating without modifying the stainless-steel surface. An elemental analysis revealed a minor residual presence of fluorine (less than 0.1%). The water contact angle for the cylinder surface after the laser treatment was found to be $53 \pm 13°$ (similar to that for the non-processed cylinders).

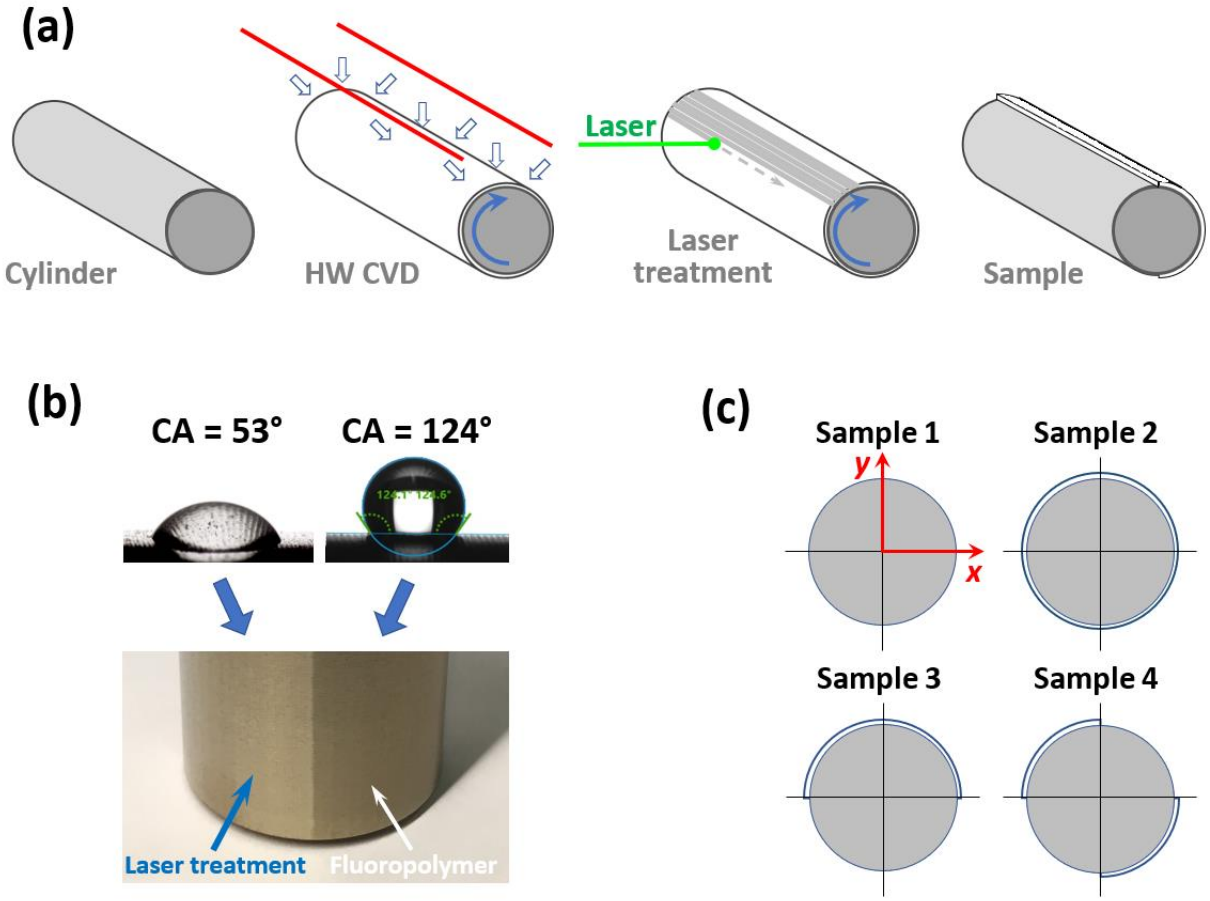

Figure 1. (a) Schematics showing the manufacturing of the samples. (b) Image of a treated cylinder, and measurement of contact angles (inserts). (c) Schematics of the tested coated samples.

Four samples are considered in the present paper: uncoated and fully coated cylinders, a sample with 180 ° sectoral removal of the coating and a sample with two opposite 90 ° sectors (Figure 1c). The details of surface morphology and elemental composition of the samples were obtained by using a HITACHI S3400N scanning electron microscope (SEM) with an Oxford Instruments INCA Energy 350 energy dispersive analyser. The surface topography was studied by a NanoScan-3D scanning probe microscope. Streamwise-oriented microscale annular groves with a depth of 5 μm and period of approximately 180 μm were observed over the untreated cylinder. The coating resulted in the formation of microstructures with a base size of about 2 – 8 μm and a height of 0.5 – 1.5 μm. Surface roughness parameters (specifically, mean deviation *Ra*, average peak-to-valley height *Rz*, root-mean-square deviation *Rms*) were estimated from the analysis of the scanned 3D profiles. Figure 2 shows the surface features before and after the coating process, with surface roughness parameters in directions along and across the groves.

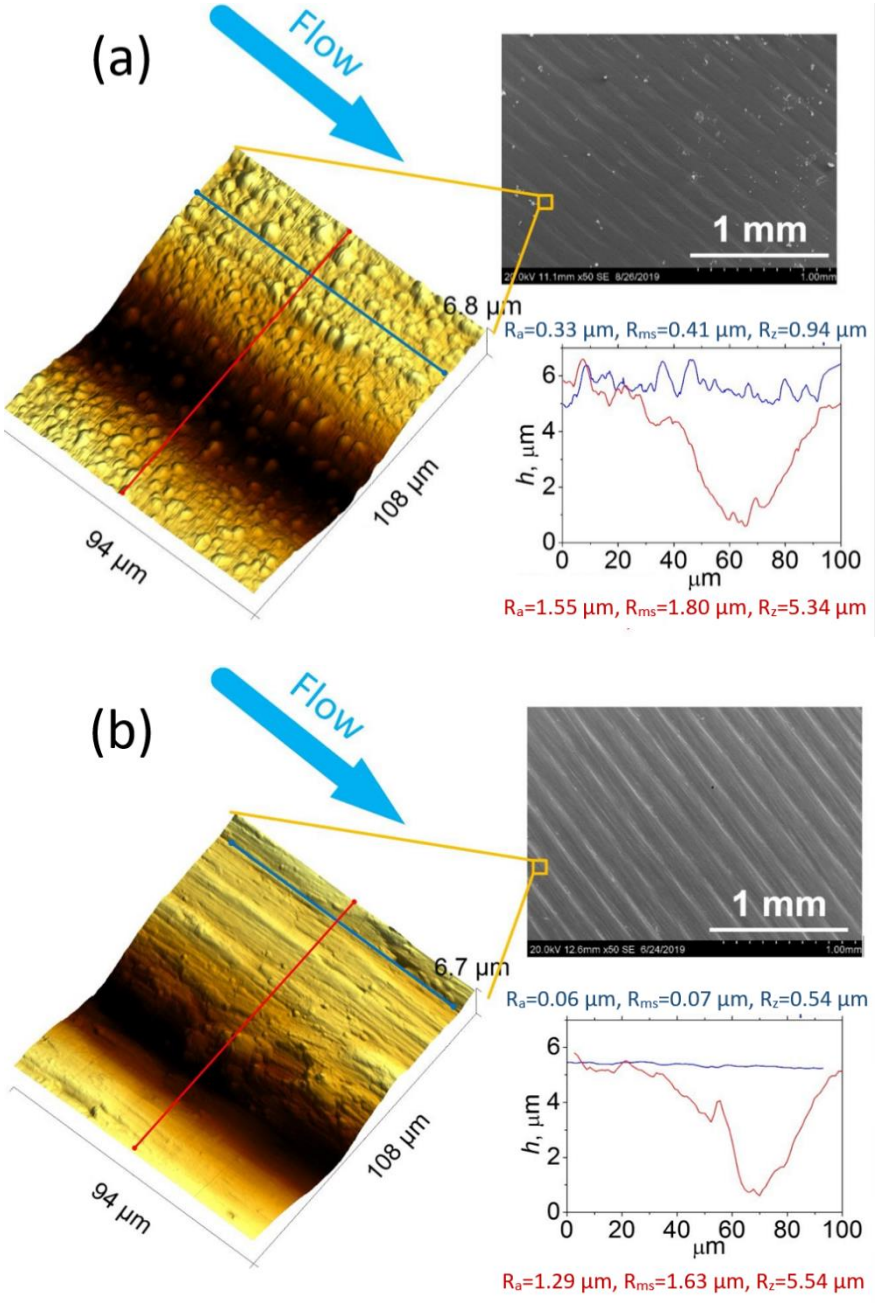

Figure 2. Images of the cylinder surface: (a) before, and (b) after laser treatment. Red and blue lines are associated with the transverse and streamwise profiles of the roughness height *h*, respectively.

The experiments were performed in a water channel (Dobrosel'skii, 2016) with a water outgassing section, cooling/heating section, honeycomb, contraction section, test section and diffuser. The facility is equipped with an ultrasonic flowmeter, temperature and pressure sensors. The water flow is driven by an electric pump, providing a bulk velocity up to 10 m/s in the transparent test section of 1 m in length with 80 × 150 mm^2 rectangular cross-section. In the present experiments, the water was filtered but not distilled or degassed to model real environments. The velocity of the flow core was set to $U_c \approx 7.8$ m/s with a fluctuation level below 1%, and the static pressure inside the channel was varied by using a special shaft section, located upstream the heat exchanger. The pressure was 1.5 kPa upstream the test section to ensure the absence of flow cavitation. The water temperature was maintained at 28 ±0.1 ℃. The concentration of dissolved air in water was approximately 0.01 m^3/m^3.

PIV measurements were performed after a few hours of continuous water channel operation at a fixed pressure and temperature to ensure equilibrium experimental conditions. The measurements were performed by using a high-repetition PIV system with two Photron V12 CMOS cameras with different optical magnification. One camera was used for the analysis of the large-scale flow dynamics in the wake region, while the second was used for high-resolution measurements (13 μm per pixel; 416 μm per vector) in the near wall region by using an Infinity K2 long-distance microscope. Velocity snapshots were evaluated by an adaptive cross-correlation algorithm. A special image segmentation was performed in the near-wall region similar to Willert (2015). Two sets of 10 000 images were captured independently for each flow case.

Figure 3 shows time-averaged velocity-field data for the four investigated flow cases. Relative to the uncoated case, the length of the recirculation zone downstream of the fully coated cylinder increases slightly from 0.62*d* to 0.83*d* due to earlier flow separation and the pulsation intensity is slightly higher. For the samples without rotational symmetry, the turbulent wake has a non-symmetric shape. Following rotation of the cylinders to obtain a mirror-reflected layer orientation, the flow structure changes in the same manner. For the sectorally coated cylinders, the turbulent wake becomes inclined towards the side on which the separation occurs earlier. The strongest increase in turbulence intensity is observed for the 90 °sectoral case. For the considered region, the integral increase of the traversal component of the turbulent kinetic energy is approximately 35% in comparison to the uncoated case.

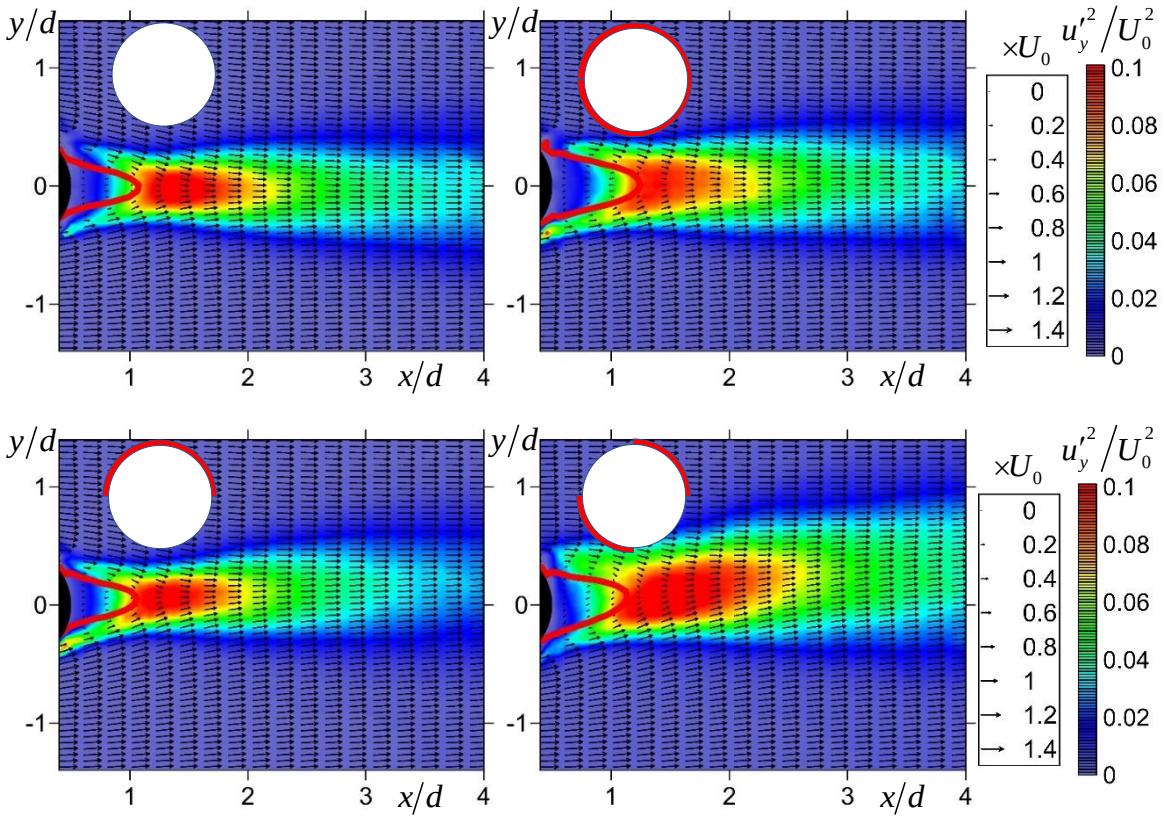

Figure 3. Mean velocity fields and local variance of the transverse velocity fluctuations. The solid line indicates the bounds of the central recirculation zone.

Figure 4 shows time-average velocity fields in the near-wall region, which allow us to evaluate the flow separation angles. For the uncoated and fully coated cylinders, the separation angle θ_{sep} (measured from the upstream stagnation point) are in the ranges 121 – 136 ° and 121 – 128 °, respectively. For the 180 ° sectoral coating case, the angle ranges are 128 – 136 ° and 122 – 129 ° on the uncoated and coated sides. For the case of 90 ° sectors, the effect is even more pronounced, viz., 124 – 132 ° and 107 – 123 ° in the coated and uncoated quarters. An almost twofold decrease in the vortex shedding frequency is also found for this case.

From the high-speed visualization it is found that micron-sized bubbles appear in the vicinity of the coated surface (cf. the uncoated and fully coated cylinders in Figure 4b, multimedia view, or two sides of the 180 °sectoral coating in Figure 4c, multimedia view). The bubbles move along the surface driven by the flow shear, and then separate above the uncoated region (see Figure 4d for the 90 °coating case, multimedia view). This suggests that gas-phase micro-layers (so-called plastron, Crisp, 1950) remain on the coated surfaces even after several hours of the continuous operation of the facility. The mechanism of micro-layer restoration warrants further investigation.

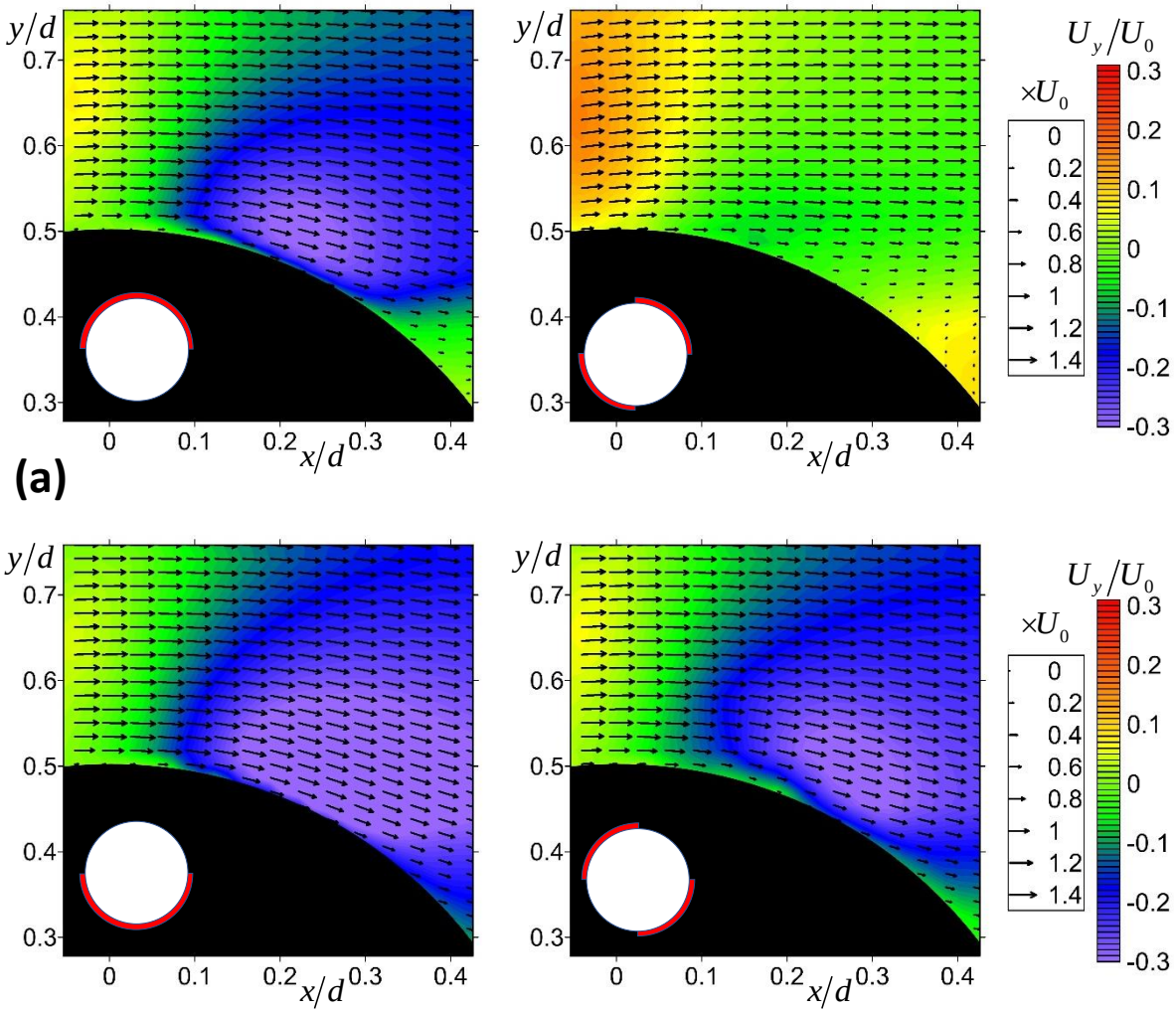

(b)

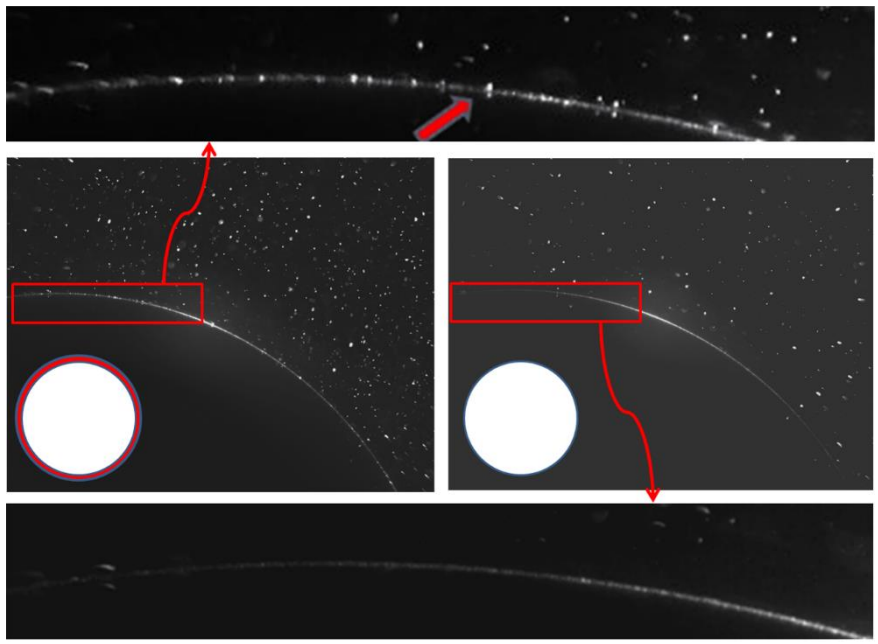

(c)

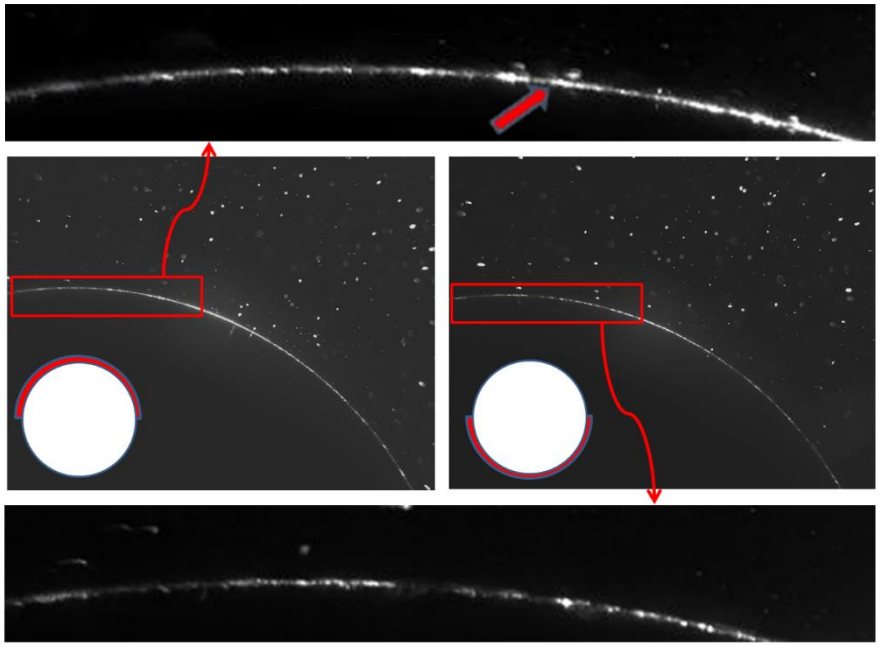

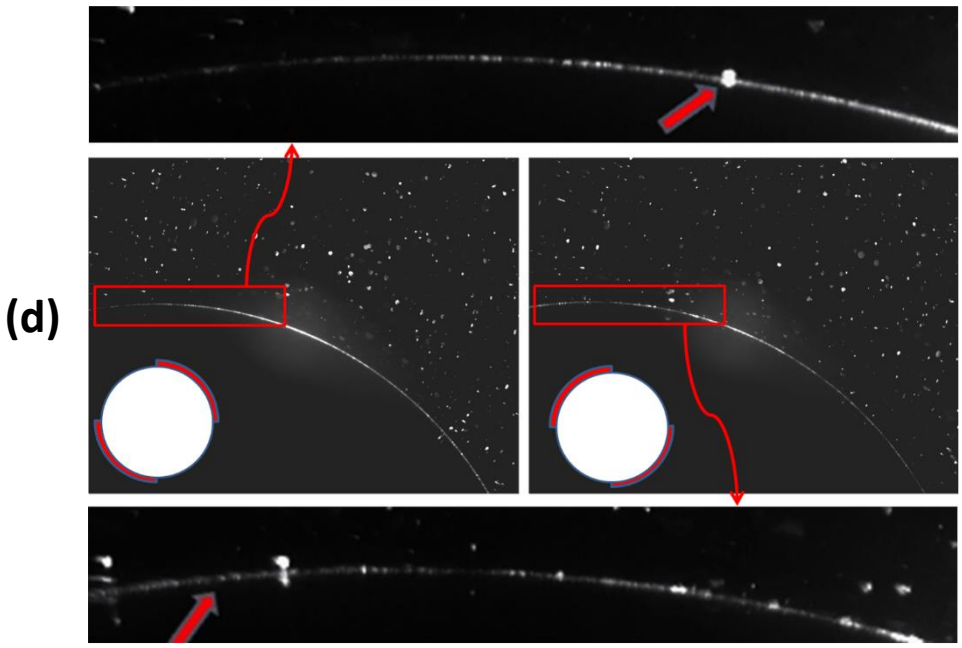

Figure 4. (a) Mean velocity field maps in the near-wall region of the sectoral coated cylinders. The magnitude of the transverse velocity component is indicated by the colour in these maps. Near-wall flow visualization videos for the (b) completely coated (left-up) and uncoated (right-bottom) cylinders (multimedia view) and for the (c) 180 ° (multimedia view) and (d) 90 ° (multimedia view) sectoral coating cases.

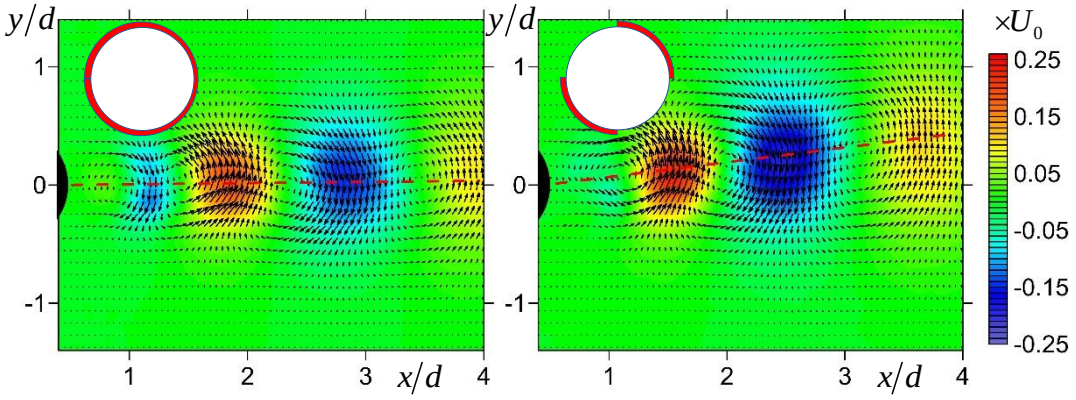

Figure 5. First two POD modes for the completely (left) and 90 °sectoral (right) coated cylinders.

Proper orthogonal decomposition (POD) is used to evaluate the kinetic energy of the velocity fluctuations (streamwise and spanwise components) associated with the global instability mode of asymmetric vortex shedding extracted by the first two POD modes. Figure 5 shows the first POD modes for two sectorally coated cases. The energy of the velocity fluctuations (in-plane components) for the fully coated cylinder increases by 16% relative to the case of the uncoated cylinder, while for the case of the 90 ° sectoral coating, the energy contained in the total and coherent turbulent fluctuations is higher by approximately 25% and 10% in comparison to the completely coated cylinder case. Furthermore, the trajectory of the coherent structures for the 90 °coating is found to be inclined by almost 6 °with respect to the upstream flow direction (3 °for the 180 °coating).

Acknowledgments

This research was funded by the Government of the Russian Federation, under Megagrant project no. 075-15-2019-1888. The examination of the samples by SEM and EDX was performed with support from the Institute of Inorganic Chemistry SB RAS (project no. FWUZ-2021-0006). The experimental facility was provided within the frame of a state contract in the Kutateladze Institute of Thermophysics. CNM acknowledges the Department for International Development (DFID) and Royal Society-DFID Africa Capacity Building Initiative, and the UK Engineering and Physical Sciences Research Council (EPSRC) [grant number EP/T03338X/1].

Data Availability

The data that support the findings of this study are available from the corresponding author upon request.

Conflicts of Interest

The authors have no conflicts to disclose.

References

Aktas, O. C., Schröder, S., Veziroglu, S., Ghori, M. Z., Haidar, A., Polonskyi, O., Strunskus, T., Gleason, K., and Faupel, F., "Superhydrophobic 3D Porous PTFE/TiO2 Hybrid Structures," Adv. Mater. Interfaces 6, 1801967 (2019). https://doi.org/10.1002/admi.201801967

Aljallis, E., Sarshar, M. A., Datla, R., Sikka, V., Jones, A., and Choi, C. H. "Experimental study of skin friction drag reduction on superhydrophobic flat plates in high Reynolds number boundary layer flow," Phys. Fluids 25(2), 025103. (2013). https://doi.org/10.1063/1.4791602

Bullee, P. A., Verschoof, R. A., Bakhuis, D., Huisman, S. G., Sun, C., Lammertink, R. G., and Lohse, D., "Bubbly drag reduction using a hydrophobic inner cylinder in Taylor–Couette turbulence," J. Fluid Mech 883, A61 (2020). https://doi:10.1017/jfm.2019.894

Bykov, N. Y., Ronshin, F. V., Safonov, A. I., Starinskiy, S. V., and Sulyaeva, V. S., "Fluoropolymer coatings deposited on rotating cylindrical surfaces by HW CVD: experiment and simulation," J. Phys. D: Appl. Phys. 54, 225204 (2021). https://doi.org/10.1088/1361-6463/abe8fd

Crisp, D. J. "The stability of structures at a fluid interface, " Trans. Faraday Soc. 46, 228-235. (1950). https://doi.org/10.1039/TF9504600228

Daniello, R. J., Waterhouse, N. E., and Rothstein, J. P. "Drag reduction in turbulent flows over superhydrophobic surfaces," Phys. Fluids, 21(8), 085103. (2009). https://doi.org/10.1063/1.3207885

Dobrosel'skii, K. G., "Use of the Piv method for investigation of motion near a cylinder in transverse flow," J. Eng. Phys. Thermophys. 89, 695–701 (2016). https://doi.org/10.1007/s10891-016-1428-2

Golovin, K. B., Gose, J. W., Perlin, M., Ceccio, S. L., and Tuteja, A., "Bioinspired surfaces for turbulent drag reduction," Philos. Trans. R. Soc. A 374, 20160189 (2016). https://doi.org/10.1098/rsta.2016.0189

Gose, J. W., Golovin, K., Boban, M., Mabry, J. M., Tuteja, A., Perlin, M., and Ceccio, S. L. Characterization of superhydrophobic surfaces for drag reduction in turbulent flow. J. Fluid Mech. 845, 560–580 (2018). https://doi:10.1017/jfm.2018.210

Huang, H., Liu, M., Gu, H., Li, X., Wu, X., and Sun, F., "Effect of the slip length on the flow over a hydrophobic circular cylinder," Fluid Dyn. Res. 50(2), 025515 (2018). https://doi.org/10.1088/1873-7005/aaab9b

Kim, N., Kim, H., and Park, H., "An experimental study on the effects of rough hydrophobic surfaces on the flow around a circular cylinder," Phys. Fluids 27, 085113 (2015). https://doi.org/10.1063/1.4929545

Kim, J., and Lee, J.S., "Surface-wettability-induced sliding bubble dynamics and its effects on convective heat transfer," Appl. Therm. Eng. 113, 639–652 (2017). http://dx.doi.org/10.1016/j.applthermaleng.2016.11.097

Legendre, D., Lauga, E., and Magnaudet, J. "Influence of slip on the dynamics of two-dimensional wakes," J. Fluid Mech. 633, 437-447. (2009). https://doi.org/10.1017/S0022112009008015

Lobasov, A. S., Alekseenko, S. V., Markovich, D. M., and Dulin, V. M., "Mass and momentum transport in the near field of swirling turbulent jets. Effect of swirl rate," Int. J. Heat Fluid Flow 83, 108539 (2020). https://doi.org/10.1016/j.ijheatfluidflow.2020.108539

Mastrokalos, M. E., Papadopoulos, C. I., and Kaiktsis, L., "Optimal stabilization of a flow past a partially hydrophobic circular cylinder," Comput. Fluids 107, 256–271 (2015). http://dx.doi.org/10.1016/j.compfluid.2014.11.010

Mastrokalos M.E., and Kaiktsis L., "Heat transfer enhancement in three-dimensional flow past a hydrophobic cylinder for heat exchanger applications," // Proceedings of the ASME 2017 Pressure Vessels and Piping Conference. Volume 4: Fluid-Structure Interaction. Waikoloa, Hawaii, USA. July 16–20, 2017. V004T04A043. ASME. https://doi.org/10.1115/PVP2017-65525

Muralidhar, P., Ferrer, N., Daniello, R., and Rothstein J.P., "Influence of slip on the flow past superhydrophobic circular cylinders," J. Fluid Mech. 680, 459–476 (2011). https://doi.org/10.1017/jfm.2011.172

Park, H., and Sun, G. "Superhydrophobic turbulent drag reduction as a function of surface grating parameters, " J. Fluid Mech. 747, 722–734. (2014). https:// doi:10.1017/jfm.2014.151

Rothstein, J. P., “Slip on superhydrophobic surfaces," Annu. Rev. Fluid Mech. 42, 89–109 (2010). https://doi.org/10.1146/annurev-fluid-121108-145558

Safonov, A. I., Sulyaeva, V. S., Gatapova, E. Y., Starinskiy, S. V., Timoshenko, N. I., and Kabov, O. A., "Deposition features and wettability behavior of fluoropolymer coatings from hexafluoropropylene oxide activated by NiCr wire," Thin Solid Films 653, 165–172 (2018). https://doi.org/10.1016/j.tsf.2018.03.015

Safonov, A. I., Kuznetsov, D. V., and Surtaev, A. S., "Fabrication of Hydrophobic Coated Tubes for Boiling Heat Transfer Enhancement," Heat Transfer Eng. 42, 1390–1403 (2020). https://doi.org/10.1080/01457632.2020.1794632

Selimefendigil, F., and Öztop, H.F., "Numerical study of MHD mixed convection in a nanofluid filled lid driven square enclosure with a rotating cylinder, " Int. J. Heat Mass Transfer 78, 741–754. (2014). https://doi.org/10.1016/j.ijheatmasstransfer.2014.07.031

Sooraj, P., Ramagya, M. S., Khan, M. H., Sharma, A., and Agrawal, A., "Effect of superhydrophobicity on the flow past a circular cylinder in various flow regimes," J. Fluid Mech. 897, (2020). https://doi.org/10.1017/jfm.2020.371

Wal, P., and Steiner, U., "Super-hydrophobic surfaces made from Teflon,"Soft Matter 3, 426–429 (2007). https://doi.org/10.1039/b613947g

Wen, J., Hu, H. B., Luo, Z. Z., and Zhang, Z. Z., "Experimental investigation of flow past a circular cylinder with hydrophobic coating, " J Hydrodynam. B 30(6), 992–1000 (2018). https://doi.org/10.1007/s42241-018-0124-4

Willert, C. E., "High‐speed particle image velocimetry for the efficient measurement of turbulence statistics," Exp Fluids 56, 1–17 (2015). https://doi.org/10.1007/s00348-014-1892-4

You, D., and Moin, P. "Effects of hydrophobic surfaces on the drag and lift of a circular cylinder, " Phys. Fluids, 19(8), 081701. (2007). https://doi.org/10.1063/1.2756578